

Electronic Supplementary Information for

***In situ* DRIFTS study of the NO + CO reaction on Fe-Co binary metal oxides over activated semi-coke supports**

Luyuan Wang<sup>a</sup>, Zhiqiang Wang<sup>a</sup>, Xingxing Cheng<sup>a,\*</sup>, Mengze Zhang<sup>a,c</sup>, Yukun Qin<sup>a,b</sup>, Chunyuan Ma<sup>a</sup>

<sup>a</sup> National Engineering Lab for Coal-fired Pollutants Emission Reduction, Shandong Provincial Key Lab of Energy Carbon Reduction and Resource Utilization, Shandong University, Jinan, China, 250061.

<sup>b</sup> School of Power Engineering, Harbin Institute of Technology, Harbin, China, 150001,

<sup>c</sup> Shandong Shenhua Shanda Energy Environment Co., Ltd, No.173 Lishan Road, Jinan, China, 250061,

\* Corresponding author: [xcheng@sdu.edu.cn](mailto:xcheng@sdu.edu.cn) (Xingxing Cheng)

## 1 Experimental methodology

### 1.2 Catalytic activity

The activity of the prepared catalysts was investigated in a fixed-bed reactor system, which consisted of a stainless steel tubular reactor (i.d. of 12.7 mm), a gas supply and flow rate control unit (mass flow meter, Beijing Sevenstar Huachuang Electronics Co., Ltd.), a gas heating unit (furnace, Shandong Lulong furnace factory), a gas analysis unit (FTIR flue gas analyzer, Gasmeter DX4000, Finland), and a data acquisition system. First, 2 g (approximately 5 cm<sup>3</sup>) of a sample was loaded in the reactor and pretreated by N<sub>2</sub> at 300 °C for 1 h, followed by cooling to room temperature. The total flow rate of the mixed gas was 500 mL/min (GHSV = 6,000 h<sup>-1</sup>). The modeled flue gas was prepared from nitrogen, 1% NO balanced by N<sub>2</sub>, and 2% CO balanced by N<sub>2</sub> (Deyang Gas Ltd.). The test under each reaction condition was completed in greater than 1 h until to a steady state, and the data were collected after the outlet concentration reached a steady state. The NO conversion and N<sub>2</sub>O selectivity were calculated from concentrations of the inlet and outlet flue gases using equations (1) and (2), respectively.

$$NO \text{ conversion} = \frac{[NO]_{in} - [NO]_{out}}{[NO]_{in}} \times 100\% \quad 1$$

$$N_2O \text{ selectivity} = \frac{2 * [N_2O]_{out}}{[NO]_{in} - [NO]_{out}} \times 100\% \quad 2$$

Where, equation (2) was transformed from the N<sub>2</sub> selectivity (equation (3)).

$$N_2 \text{ Selectivity} = \left( 1 - \frac{2[N_2O]_{out}}{[NO_x]_{in} - [NO_x]_{out}} \right) \times 100\% \quad 3$$

### 1.3 Catalyst characterization

The textural properties were evaluated by the physical adsorption of  $N_2$  at 77 K using an automatic surface analyzer (Quantachrome Autosorb 1C), and the specific surface areas and pore volumes were calculated using density functional theory (DFT) from the  $N_2$  adsorption/desorption isotherm. XRD patterns were recorded on a Rigaku D/max 2400 diffractometer using Cu-K $\alpha$  radiation ( $\lambda = 1.5056 \text{ \AA}$ ) at a scanning rate of  $8^\circ/\text{min}$  with a step size of  $0.02^\circ$  over the  $2\theta$  range of  $10\text{--}80^\circ$ . The surface morphologies of the samples were observed by field-emission scanning electron microscopy (SEM, Hitachi S-4800).

## 2 Results

### 2.1 XRD and Raman analysis

The XRD results of three representative catalysts ( $Fe_{0.8}Co_{0.2}/ASC$ ,  $Fe_{0.8}/ASC$  and  $Co_{0.2}/ASC$ ) were presented in Fig. S1. For all the catalysts, there was a diffraction peak in about  $25\text{--}30^\circ$ , which is a characteristic peak for graphite's (002) crystal face (JCPDF=13-0148). This characteristic peak declined with an increment of metal loading. Noteworthy, characteristic peaks of iron oxides and cobalt oxides are not observed for  $Fe_{0.8}Co_{0.2}/ASC$ , but an obvious peak of  $CoFe_{15.7}$  (JCPDF=65-7519) was found. It was thus confirmed that there is a mixed crystal effect in the co-impregnation process. In the XRD pattern of  $Fe_{0.8}/ASC$ , some characteristic peaks for iron species were detected, such as  $Fe_2O_3$  (JCPDF=24-0072),  $FeO$  (JCPDF=03-0968) and  $Fe$  (JCPDF=01-1262). While for  $Co_{0.2}/ASC$ , characteristic peaks of  $CoO$  (JCPDF=48-1719) and zero valent  $Co$  (JCPDF=15-0806) appeared. No other peaks for cobalt species were further found.

### 2.2 Catalytic performance

Catalysts with different metals were prepared and their catalytic activities of NO reduction by CO were presented in Fig. S2. For all the prepared catalysts, the NO reduction efficiency increased with temperature. In Fig. S2(a), it could be found that  $Fe_{0.8}Co_{0.2}/ASC$  catalyst exhibited the best deNO activity and thus was selected for the further discussion of reaction mechanisms. Notably, about 100% NO conversion could be achieved over the selected  $Fe_{0.8}Co_{0.2}/ASC$  catalyst at a temperature as low as  $200^\circ\text{C}$ .

For the NO reduction, NO could be reduced to either  $N_2O$  or  $N_2$ . The  $N_2O$  selectivity of different catalysts and at different temperatures was presented in Fig. S2(b). At temperatures at and lower than  $150^\circ\text{C}$ , most of the converted NO was reduced to  $N_2O$ , instead of the harmless  $N_2$ . Thus the prepared ASC catalysts should be used at temperatures above  $200^\circ\text{C}$ . For most catalysts, the  $N_2O$  selectivity exhibited an opposite trend to NO conversion. The higher the deNO activity, the lower the  $N_2O$  selectivity. Zero  $N_2O$  selectivity, that is 100% reduction to  $N_2$ , was achieved by the  $Fe_{0.8}Co_{0.2}/ASC$  catalyst at  $200^\circ\text{C}$ .

### 2.3 Surface morphology of catalysts

Fig. S3 presented the surface morphologies of some representative catalysts, *i.e.*,  $\text{Fe}_{0.8}\text{Co}_{0.2}/\text{ASC}$ ,  $\text{Fe}_{0.8}/\text{ASC}$ ,  $\text{Co}_{0.2}/\text{ASC}$  and ASC. The surface of activated semi-coke support showed a carbon foliated structure. When Fe was loaded onto the ASC support, the  $\text{Fe}_{0.8}/\text{ASC}$  catalyst showed a block-like structure, with clusters of metal oxides aggregated on surface<sup>2</sup>. The morphology of  $\text{Co}_{0.2}/\text{ASC}$  was quite different, presenting a dispersed leaf-like structure, and analogous morphology was proposed by previous literature<sup>3, 4</sup>. When both Fe and Co were impregnated, big spherical clusters could be observed on the surface. The surface morphology was significantly changed by co-impregnation of Co and Fe. It is speculated that this special spherical structure may be ascribed to the mixed crystal effect<sup>5</sup>.

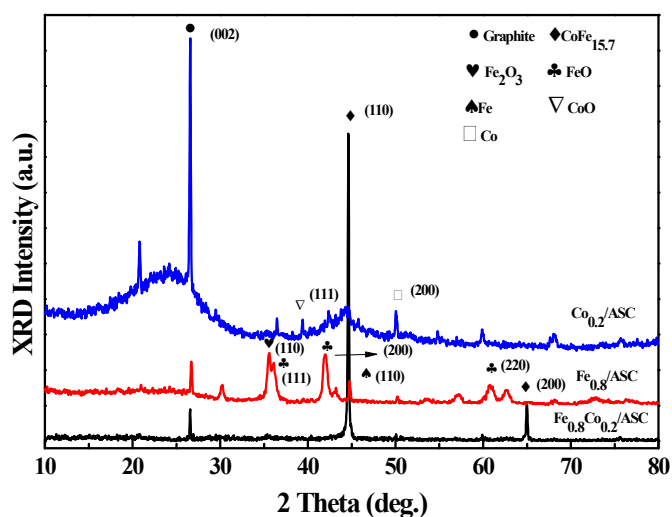


Fig. S1 XRD patterns of catalysts

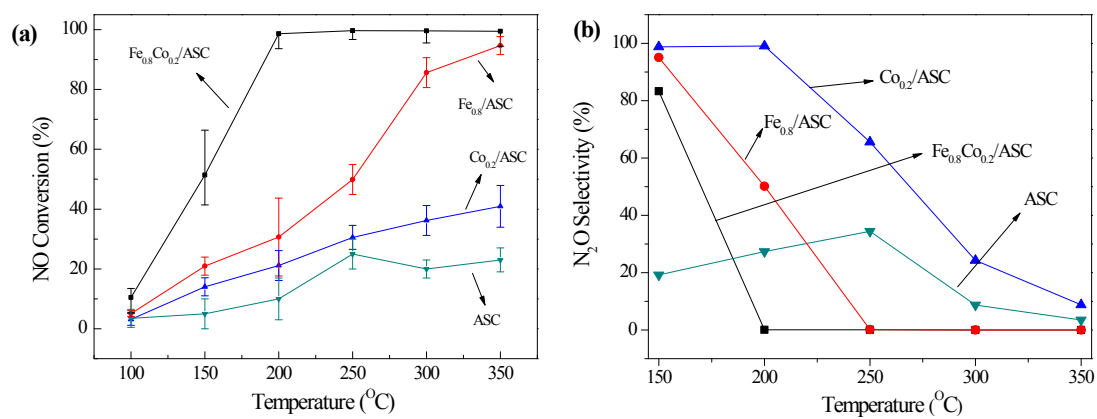


Fig. S2 NO conversion (a) and  $\text{N}_2\text{O}$  selectivity (b) of catalysts in the reduction of NO. Reaction conditions: 2000 ppm CO, 1000 ppm NO and balance  $\text{N}_2$ , GHSV=6,000  $\text{h}^{-1}$ .

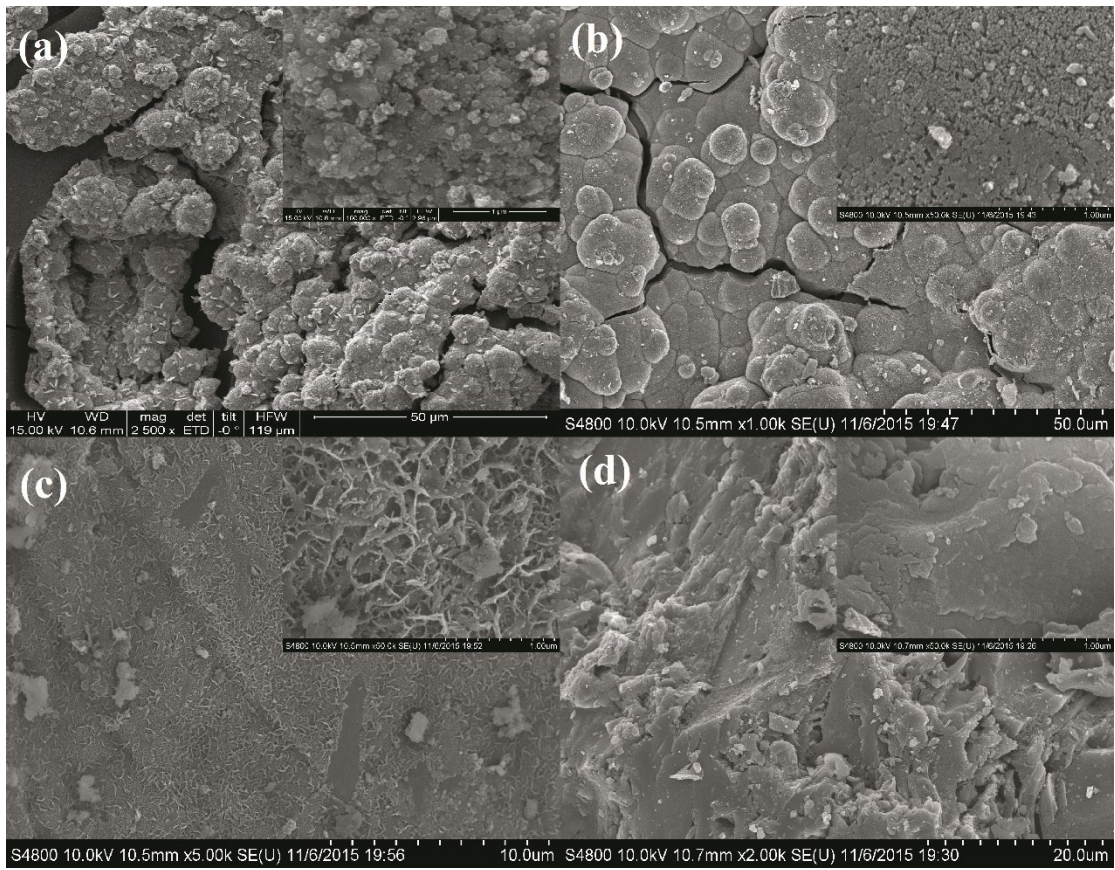


Fig. S3 SEM images of catalysts (a) ASC, (b)  $\text{Fe}_{0.8}\text{Co}_{0.2}/\text{ASC}$ , (c)  $\text{Fe}_{0.8}/\text{ASC}$  and (d)  $\text{Co}_{0.2}/\text{ASC}$ .

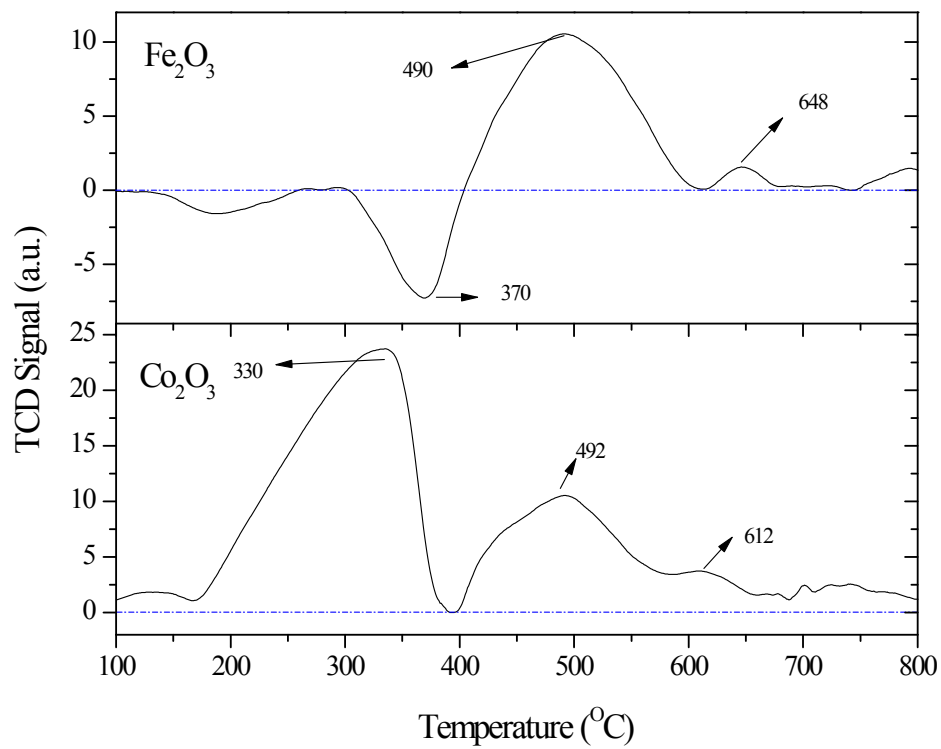


Fig. S4 CO-TPR profiles of pure metal oxides.

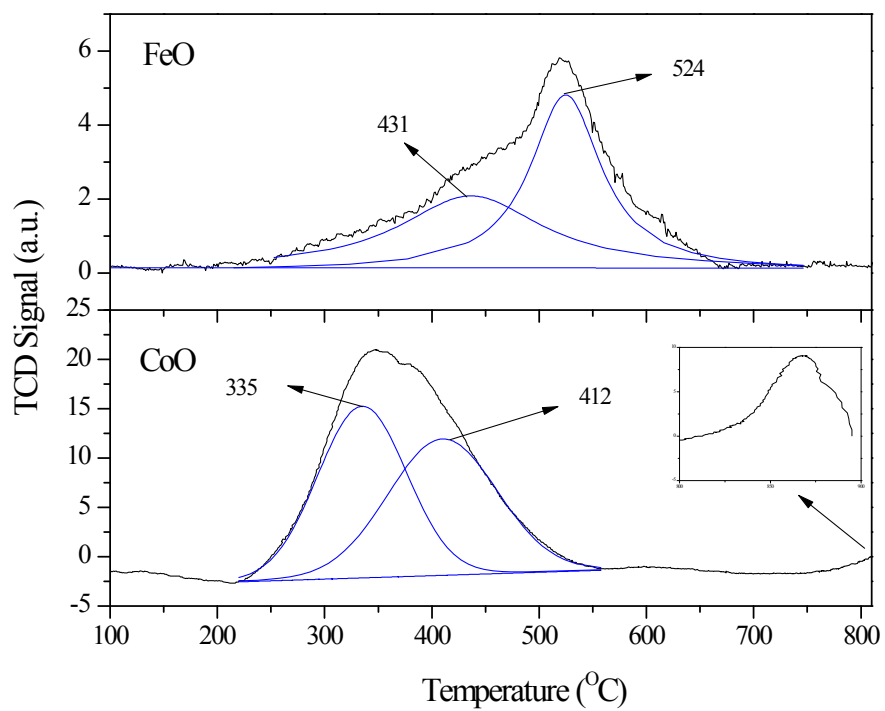


Fig. S5 NO-TPO profiles of pure metal oxides.

## Reference:

1. L. Simonot and G. Maire, *Applied Catalysis B: Environmental*, 1997, **11**, 181-191.
2. L. Dong, B. Zhang, C. Tang, B. Li, L. Zhou, F. Gong, B. Sun, F. Gao, L. Dong and Y. Chen, *Catal. Sci. Technol.*, 2014, **4**, 482-493.
3. F. Wu, X. Ma, J. Feng, Y. Qian and S. Xiong, *Journal of Materials Chemistry A*, 2014, **2**, 11597-11605.
4. J. Jiang, J. Liu, R. Ding, X. Ji, Y. Hu, X. Li, A. Hu, F. Wu, Z. Zhu and X. Huang, *The Journal of Physical Chemistry C*, 2009, **114**, 929-932.
5. S. Nishigaki, S. Yano, H. Kato, T. Hirai and T. Nonomura, *Journal of the American Ceramic Society*, 1988, **71**.